Mechanics of Advanced Composite Structures

Journal homepage: https://macs.semnan.ac.ir/

Semnan University

ISSN: 2423-7043

Research Article

Experimental Investigation and RSM-Based Optimization of Phenolic/PTFE/SiC Composites

Milad Aghalari, Reza Azarafza *, Jafar Eskandari Jam

Ali Davar, Amir Kaveh

Faculty of Materials and Manufacturing Technologies, Malek Ashtar University of Technology, Tehran, Iran

ARTICLE INFO

Article history:

Received:
Revised:
Accepted:

Keywords:

Resole;
Polytetrafluoroethylene;
Silicon carbide;
D-Optimal algorithm;
hybrid laminates

ABSTRACT

Resole phenolic resin, valued for its excellent heat resistance, strong adhesion, and chemical stability, has long been utilized in aerospace, automotive, and protective material applications. However, its relatively low toughness and brittleness limit broader use. In this study, the thermal and mechanical characteristics of phenolic composites were improved by incorporating Polytetrafluoroethylene (PTFE) powder, Silicon carbide (SiC) particles, carbon, and high-silica fibers. A D-optimal response surface methodology (RSM) design was employed to evaluate the effects of fiber type, curing temperature, and particle loading. Scanning electron microscopy (SEM) analysis revealed that the addition of reinforcing particles altered fracture morphology by promoting crack deflection and improving resin–fiber interaction. Differential scanning calorimetry (DSC) results confirmed a 7% increase in glass transition temperature (Tg) with 10% particle loading, indicating enhanced thermal stability. Mechanical testing demonstrated that the addition of 10 wt% reinforcing particles enhanced both tensile and flexural properties, regardless of the fiber type; however, the fiber type itself had a significant influence on performance. Carbon fiber composites achieved the highest tensile strength (264.8 MPa), which was 13% above hybrid laminates (235.2 MPa) and 185% above high-silica composites (93.0 MPa). Conversely, hybrid laminates exhibited the best flexural strength (219.9 MPa), exceeding carbon by 72% and high-silica by 150%. Quantitative ANOVA validation confirmed the reliability of the developed models for both tensile and flexural strength. Optimal parameters—10% particle loading, 180°C curing with carbon fibers for tensile strength, and hybrid fibers for flexural strength—offer clear, actionable guidance for industrial applications.

1. Introduction

Polymers are mainly categorized into two main types: thermoset and thermoplastic polymers [1]. Among thermoset resins, phenolic resins have widespread applications across various industries, including automotive, adhesive manufacturing, and aerospace, due to their favorable properties such as excellent thermal resistance, electrical insulation, and good chemical resistance [2, 3]. Phenolic resins can be divided into two categories: novolac and resole. Novolac resins have a molar ratio of formaldehyde to phenol that is less than one, requiring a curing agent for hardening. In contrast, resole resins have a molar ratio of formaldehyde to phenol greater than one (typically around 1.5), allowing them to cure directly due to their inherent reactivity [3, 4]. It is important to note that phenolic resins alone do not possess strong physical and mechanical properties; they tend to be brittle with low tensile and flexural strength when unreinforced. Therefore, to enhance their performance and make them suitable for engineering applications, it is essential to incorporate reinforcing materials, such as fibers or particles, into the resin [1, 2, 5, 6].

* **Corresponding author.**
E-mail address: azarkntu@yahoo.com

High-silica fibers are among the reinforcing materials that demonstrate excellent mechanical and thermal properties, making them suitable for use as a reinforcing phase in resin. These fibers have a wide range of applications in the aerospace, automotive, and construction industries [7]. Research by Wei et al. has shown that the use of silica needle fibers enhances the mechanical properties of silica composites, including tensile strength, compressive strength, and flexural strength [8]. Additionally, research by Li et al. indicates that phenolic/silica composites have low thermal conductivity, which makes them effective for thermal protection [9].

Carbon fibers are among the most widely used reinforcing fibers in various industries. Carbon fiber reinforced composites offer significant advantages due to their low density, high strength, and stiffness. These composites feature low thermal expansion, high thermal stability, and excellent resistance to creep, fatigue, and corrosion [10-12]. Rahmani et al. examined the mechanical performance of epoxy/carbon fiber composites, finding that optimal fiber orientations and increased layer counts enhance both tensile and flexural strengths, while carbon fibers also improve the load-bearing capacity [13].

Filler particles are an essential aspect of reinforcements that enhance the properties of composites [14]. For example, additives significantly enhance the properties of polymer composites, improving fracture behavior and energy absorption in flexible hybrid biocomposites with rubber/biofiller layers [15], mechanical strength in cellulose nanofiber-reinforced elastomers [16], impact resistance in lignin-filled natural rubber/hemp composites [17,18], and sensing capabilities in carbon nanotube-polyurethane acrylate systems [19].

One of the fillers, Polytetrafluoroethylene (PTFE) powder, stands out due to its unique characteristics, such as high thermal resistance and excellent chemical resistance [20]. Zhangande et al. demonstrated in their research that incorporating PTFE powder into POM polymer leads to a reduction in tensile strength but a significant increase in impact strength [21]. Similarly, Paninande et al. investigated the effects of adding PTFE particles to polyimide polymer. They found that in polyamide composites, the combination of PTFE particles with annealed carbon fibers improves wear resistance and doubles the elastic modulus compared to pure Polyimide [22]. In another study, Basavarajande et al. reported that increasing the proportion of PTFE particles in Nylon 66 polymer enhances the stability and thermal properties of the composite [23]. In addition to being used as a filler, PTFE itself can also be used as a matrix in the manufacture of sealing composites. For instance, Daneshmand et al. demonstrated that incorporating Inconel 625 alloy powder into PTFE matrices enhances wear resistance, corrosion properties, and sealing performance [24].

Silicon carbide (SiC) is one of several additives that can enhance the thermal and mechanical properties of polymers [25, 26]. Basingala et al. demonstrated in their study that incorporating SiC powder into phenolic/carbon composites results in improved strength and flexural modulus. The most significant enhancements were observed in samples with 3% SiC, where the flexural strength increased by 12% and the flexural modulus by 7% [27]. Additionally, Kasmaei and colleagues investigated the impact of adding SiC and ZrB2 particles to novolac-epoxy/carbon composites. Their findings indicated that the combined addition of SiC and ZrB2 improves both erosion resistance and mechanical strength [28].

The use of experimental design methods is highly effective in reducing research time and costs [29]. Various techniques, such as response surface methodology (RSM) and the Taguchi method, are particularly suitable for experiments involving a large number of significant parameters [30]. RSM encompasses a set of mathematical and statistical procedures that aid in the development, refinement, and optimization of processes [31]. Among the methods employed in RSM are central composite design (CCD), Box–Behnken design (BBD), and D-optimal design [29]. Unlike BBD and CCD, which only accommodate quantitative variables in experimental design, the D-optimal design method allows for the inclusion of both quantitative and qualitative variables [۳2, ۳3]. Daneshpayeh et al. investigated the mechanical properties of polypropylene linear/low-density polyethylene nanocomposites reinforced with titanium nanoparticles using response surface methodology within the Box–Behnken design. They discovered that an RSM significantly reduced the number of required experiments compared to classical factorial designs and produced statistically reliable models for predicting and optimizing composite properties [۳4]. Additionally, Yaghoubi and Fereydoun optimized a polypropylene nanocomposite reinforced with kenaf fibers using the response surface methodology within the Box–Behnken design. Their study revealed that RSM was employed to establish second-order regression models linking fiber content and processing variables to mechanical responses, and ANOVA confirmed the statistical validity of the models (high R^2 and insignificant lack-of-fit). The approach not only reduced the number of

required experiments compared with full factorial designs, but also enabled precise determination of optimal parameter levels for maximizing tensile performance [٣5].

Based on findings from previous studies, this research employed the RSM experimental design method, utilizing the D-optimal algorithm, to optimize the variables. The percentage of PTFE and SiC reinforcing particles in resole-based phenolic composites, as well as the curing temperature, were selected as quantitative variables. At the same time, the type of fibers was chosen as a qualitative variable. The tensile and flexural mechanical properties, Differential Scanning Calorimetry (DSC) tests, and microscopic morphology were examined in this study. The main aspect of the distinction and innovation of this study from previous studies is that its main goal is to show the effect of different parameters on the properties of the resole composite and how they interact with each other. The use of silicon carbide and PTFE particles, along with the design of experiments that incorporate both quantitative and qualitative variables, is a key aspect of this research.

2. Experimental Method

2.1. Materials

In this research, a resole-based phenolic resin, identified as IL800, with a viscosity ranging from 600 to 800 mPa·s, was provided by Resitan Company. To reinforce the resin, 300 grams of plain weave carbon fiber and 300 grams of plain weave high-silica fiber were employed. Additionally, PTFE powder with a particle size of 1 μm, manufactured by Tianwax company in South Korea, and SiC powder with a particle size of 5 μm from Sanhui Chinese company were incorporated to enhance the properties of the composite. The properties of the materials used in this research are summarized in Table 1.

Table 1. Properties of Materials

Material	Properties
Resole resin	viscosity 600-800 mPa.s
	density 1.21 g/cm^3
Carbon fiber	weight 300 g/m^2
	weave Plain
	density 1.78 g/cm^3
High-silica fiber	weight 300 g/m^2
	weave Plain
	density 1.84 g/cm^3
PTFE particle size	1 micron
SiC particle size	5 micron

2.2. Production of Samples

The composite contained approximately ٧٠ wt.% fiber reinforcement (either carbon, high-silica, or hybrid) and ٣٠ wt.% resin matrix. The PTFE and SiC powders were first weighed to the target fraction and gradually introduced into the phenolic resin under mechanical stirring at 1000 rpm for 15 minutes to ensure uniform dispersion. Next, fibers were impregnated with the resin and manually placed into a mold. The dimensions of the tensile mold were 255×80×2.5 mm^3, while the dimensions of the flexural mold were 155×80×3 mm^3.

Each laminate consisted of ten plies of woven fabric. For hybrid configurations, carbon and high-silica fabrics were alternately stacked in a symmetric sequence (five plies of carbon and five plies of high-silica). The vacuum bag molding method was employed to remove excess resin and air bubbles, using a standard configuration of peel ply, release film, and breather fabric. The layup was subjected to a vacuum for 1 hour (~0.08 MPa) to ensure air removal and uniform compaction. After vacuuming, the laminate, without the bag, was placed inside the hot press, where curing was carried out at the specified temperatures (140 °C, 160 °C, or 180 °C) for 4 hours under 150 psi(~10 bar). To minimize thermal stresses, post-curing was performed in an oven for 1 hour, with the temperature gradually increasing from 100 °C to 160 °C in 20 °C increments, followed by controlled cooling within the oven. The cured composite sheets were then cut into standard dimensions for tensile and flexural tests using a waterjet machine. The weight of each tensile specimen was 25 to 35 grams, and the weight of each flexural specimen was about 20 to 25 grams. The overall manufacturing process is schematically illustrated in Fig. 1.

2.3. Scanning Electron Microscope Test

To examine the morphology of the fractured samples, a MIRA3 field-emission scanning electron microscope (FE-SEM) manufactured by Tescan was used. It features a Schottky emitter, enabling high-resolution imaging with a resolution of 1.2 nm at 30 kV. The samples were coated with a thin layer of gold and tested under controlled laboratory conditions at 20°C and ٥0% humidity.

2.4. Differential Scanning Calorimetry test

Differential Scanning Calorimetry (DSC) was conducted using a TA Instruments Q2000 under a nitrogen atmosphere, with a heating rate of 10 °C/min in the temperature range of 25–٢00 °C. Small cured composite specimens (approximately 5–10 mg) were cut from molded panels after post-curing for DSC analysis. The goal was to determine the glass transition

temperature (Tg) and evaluate how fillers and fiber type influence cross-linking density.

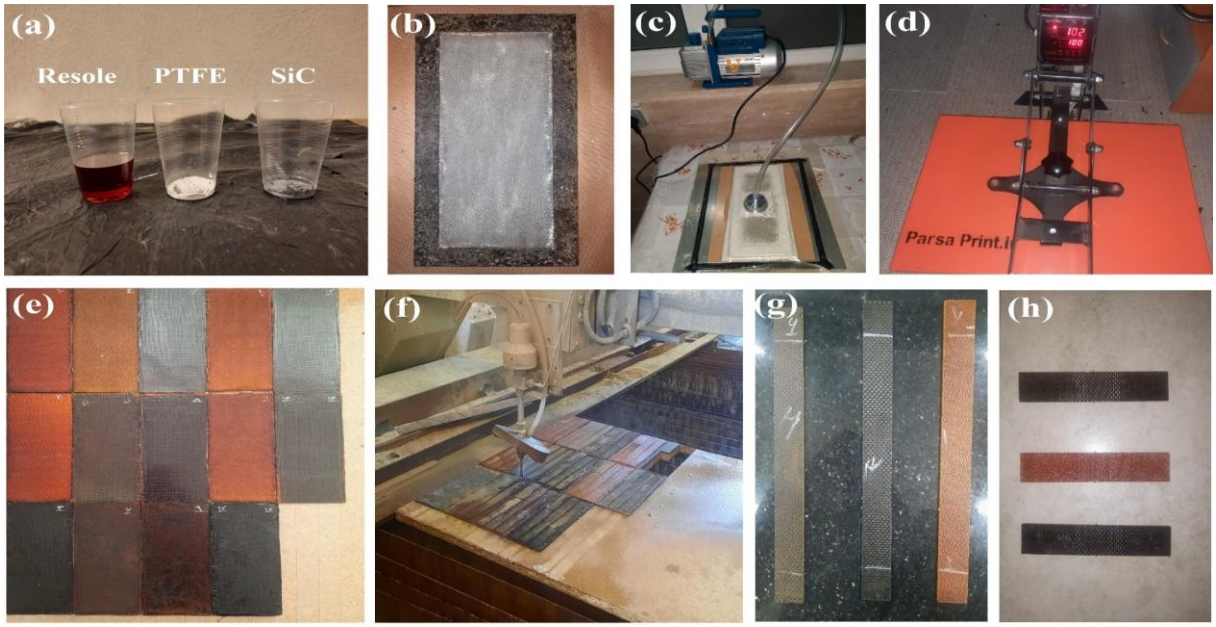

Fig. 1. (a) Materials before mixing, (b) Fiber impregnation with mixing materials and molding , (c) Vacuum bagging configuration consisting of peel ply, release film, and breather, (d) Hot press curing, (e) Prepared Samples before cutting, (f) Waterjet cutting for tensile and flexural samples, (g) Tensile Samples, (h) Flexural Sample

2.5. Tensile and Flexural Tests

Tensile specimens were prepared from the fabricated sheets according to the ASTM D3039 standard, with dimensions of 250 × 25 × 2.5 mm^3. Tensile tests were conducted on each specimen using a Gotech machine with a capacity of 20 tons, made in Taiwan, at a speed of 2mm/min.

For the flexural tests, specimens were prepared according to the ASTM D790 standard, with dimensions of 150×25×3 mm^3. These flexural tests were performed using a Gotech universal machine, also made in Taiwan, at a speed of 2mm/min and with a support span of 50 mm.

To minimize errors, each test was repeated three times for each specimen, and the average results are reported.

3. Experimental Design

Response Surface Methodology (RSM) is a modern and widely used approach for optimizing parameters to achieve maximum mechanical properties. This method evaluates the effect of parameters and their interactions on mechanical responses, along with analyzing variance, to predict mechanical properties using mathematical models. Two-dimensional and three-dimensional diagrams of response surfaces can facilitate this prediction.

In most cases involving RSM, the relationship between the response and the input variables is not known. Thus, the first step is to find a suitable approximation of the actual relationship between the response variable (y) and the set of independent variables (x). The prediction of mechanical properties is based on a mathematical model that considers the influence of each independent variable, its squares, and the interactions among them. This prediction can be expressed using the following polynomial equation [30, 34].

$$= \beta_0 + \sum_{i=1}^{k} \beta_i x_i + \sum_{i=1}^{k} \beta_{ii} x_i^2 + \sum_{i} \sum_{j} \beta_{ij} x_i x_j + \varepsilon \quad (1)$$

In the above function, x_i and x_j are input variables, β_0 is a constant value, β_i is a linear coefficient, β_{ii} is a quadratic coefficient, β_{ij} is an effect interaction coefficient, k is the number of independent variables, y is the response, and ε is the observed error value [30].

In this study, based on previous research, two quantitative parameters were selected: additive weight percentage (Pw) and curing temperature (T), each evaluated at three levels. Additionally, the fiber type parameter (F) was chosen as a qualitative parameter, also assessed at three levels. These parameters were defined as input variables. Table 2 presents the selected parameters along with their corresponding values, while Table 3 displays the experiments designed using Design-Expert software. For reinforcement, a combination of PTFE and SiC particles was used along with carbon and high-silica fibers.

According to Table 3, the Design-expert software suggests 14 samples for mechanical

tensile and flexural tests, and the values of each parameter for each sample are specified in Table 3. After performing the necessary tests on 14 samples, statistical analysis of the obtained results was performed using the ANOVA method and the D-optimal algorithm.

Table 2. Experimental factors and their range of variation

Factor Name	Symbol	Unit	Level 1	Level 2	Level 3
Particle Weight	P	wt.%	0	5% (2.5% PTFE+2.5%SiC)	10% (5% PTFE+5%SiC)
Cure Temperature	T	℃	140	160	180
Fiber	F	-	Carbon	Highsilica	Carbon/Highsilica

Table ٣. Design of tests based on D-optimal

Sample	Particle weight (wt.%)	Temperature (℃)	Fiber
1	0	180	Highsilica
2	0	140	Highsilica
3	5	180	Carbon
4	10	180	Highsilica
5	10	140	Carbon/Highsilica
6	10	180	Carbon/Highsilica
7	10	160	Carbon
8	0	140	Carbon/Highsilica
9	5	140	Carbon
10	5	160	Highsilica
11	5	140	Highsilica
12	0	160	Carbon
13	0	180	Carbon/Highsilica
14	10	140	Carbon/Highsilica

4. Results and Discussion

4.1. SEM Test

A scanning electron microscope (SEM) examination was conducted on the fracture cross-section of samples 1, 4, 6, 7, 12, and 13 (refer to Table 3). Among these samples, three are composite samples without reinforcing particles (samples 1, 12, and 13), while the other three contain reinforcing particles (samples 4, 6, and 7).

Analyzing the microstructure of the composite samples provides valuable insights into the arrangement of the fibers and matrix, as

As well as the distribution of the particles within the matrix.

Debonding, pull-out, and fiber failure are among the failure mechanisms in composites [36]. Fiber failure is generally preferred in composites because the fibers possess higher tensile strength. When stress is applied to the composite, it is transferred to the fibers, enabling the material to bear greater loads. Additionally, fiber failure suggests strong adhesion between the fibers and the matrix. [37, 38]. Fiber failure typically initiates gradually through the development of small cracks, allowing the composite structure to exhibit warning signs before complete failure occurs. Moreover, fibers contribute to a uniform distribution of stress throughout the composite, which diminishes the likelihood of abrupt failure [37, 39-٤1].

SEM observations revealed distinct failure mechanisms between high-silica and carbon fiber composites (Fig. 2). In the case of high-silica laminates, as shown in Fig. 2(a) and Fig. 2(b), interfacial debonding and extensive fiber pull-out were evident, indicating poor adhesion between the silica fibers and the phenolic matrix. Such failure modes prevent efficient stress transfer, explaining why the tensile strength of these composites (~67 MPa, Table 5) remains close to that of the pure phenolic resin. By contrast, the carbon fiber composites in Fig. 2(c) and Fig. 2(d) exhibited a different morphology. Although some fiber pull-out was observed, some fibers showed clear fiber fracture with broken ends embedded in the matrix. Fiber fracture is generally considered a more favorable mode of failure, as it implies stronger fiber–matrix bonding and more effective load transfer to the fibers, thereby enabling much higher tensile strength (~265 MPa, Table 5). This comparison confirms that the weak interface in silica-based composites limited reinforcement, while the stronger bonding in carbon fiber laminates contributed to their superior mechanical performance.

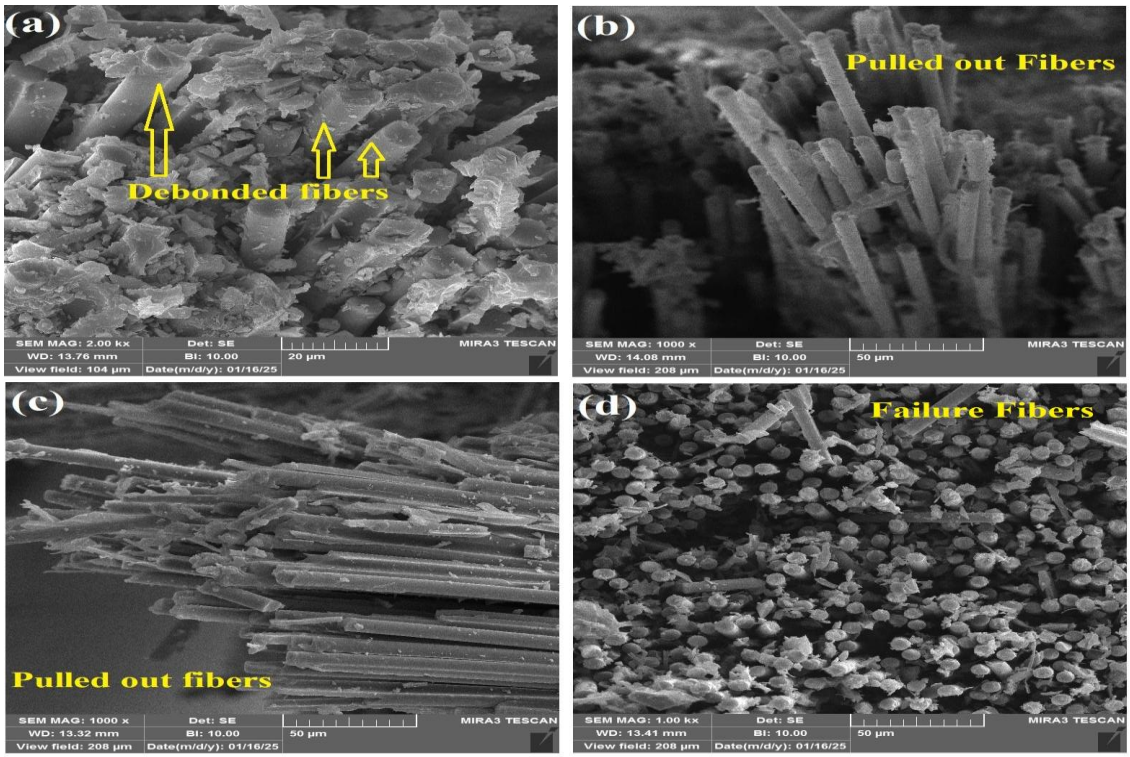

Fig. 2. (a) Highsilica fibers with 2000x magnification, (b) Highsilica fibers, (c) Carbon fibers, (d) Carbon fibers with 1000x magnification

Fig. 3(a) and Fig. 3(b) display the fracture surfaces of samples without reinforcing particles, while Fig. 3(c) and Fig. 3(d) illustrate the fracture surfaces of samples reinforced with particles. The differences between these two types of samples are pretty noticeable.

The fracture surfaces of the samples without reinforcing particles appear rougher compared to those with reinforcing particles. This roughness may be attributed to the fact that, in these samples, the matrix and fibers alone bear the applied stress, resulting in fractures that create a rough and layered surface. In contrast, the fracture surfaces of the samples containing reinforcing particles are smoother and more homogeneous. This softer surface can be attributed to the reinforcing particles' ability to enhance the resin structure, thereby preventing the matrix from fracturing and inhibiting the growth and spread of cracks. As a result, stress is distributed more uniformly across the entire composite surface. Furthermore, the fracture surfaces of the samples shown in Fig. 3(a) and Fig. 3(b) exhibit tiny holes, which can lead to composite failure and indicate inadequate adhesion between the fibers and the matrix. In contrast, Fig. 3(c) and Fig. 3(d) demonstrate that the presence of reinforcing particles results in a more uniform composite structure, fewer holes, and improved adhesion between the matrix and fibers. This enhancement contributes positively to the overall toughness of the structure.

However, occasional particle agglomeration was also observed, which may locally weaken the matrix. Nevertheless, the overall comparison highlights that the incorporation of SiC and PTFE substantially alters the fracture morphology compared to particle-free samples, leading to improved adhesion and effective crack-arresting mechanisms. These microstructural features directly explain the enhanced tensile and flexural performance observed in Table 5, confirming that particle-reinforced laminates exhibit higher load-bearing capacity and delayed failure. Overall, the SEM analysis demonstrates that the addition of SiC and PTFE not only changes the fracture surface morphology but also provides the underlying mechanism for the superior mechanical behavior of the developed phenolic-based composites.

Fig. 4 displays SEM images of high-silica fibers, carbon fibers, PTFE particles, and SiC particles. In Fig. 4(a), the high-silica fibers have an approximate diameter of 9 µm, while in Fig. 4(b), the carbon fibers measure around 7 µm in diameter. Additionally, Fig. 4(c) shows that the PTFE particles are approximately 2.5 µm in size, and Fig. 4(d) indicates that the SiC particles are around 5 µm. One reason some particles might appear larger than the initial sizes listed in Table

1 is that the resin can be absorbed by the additive

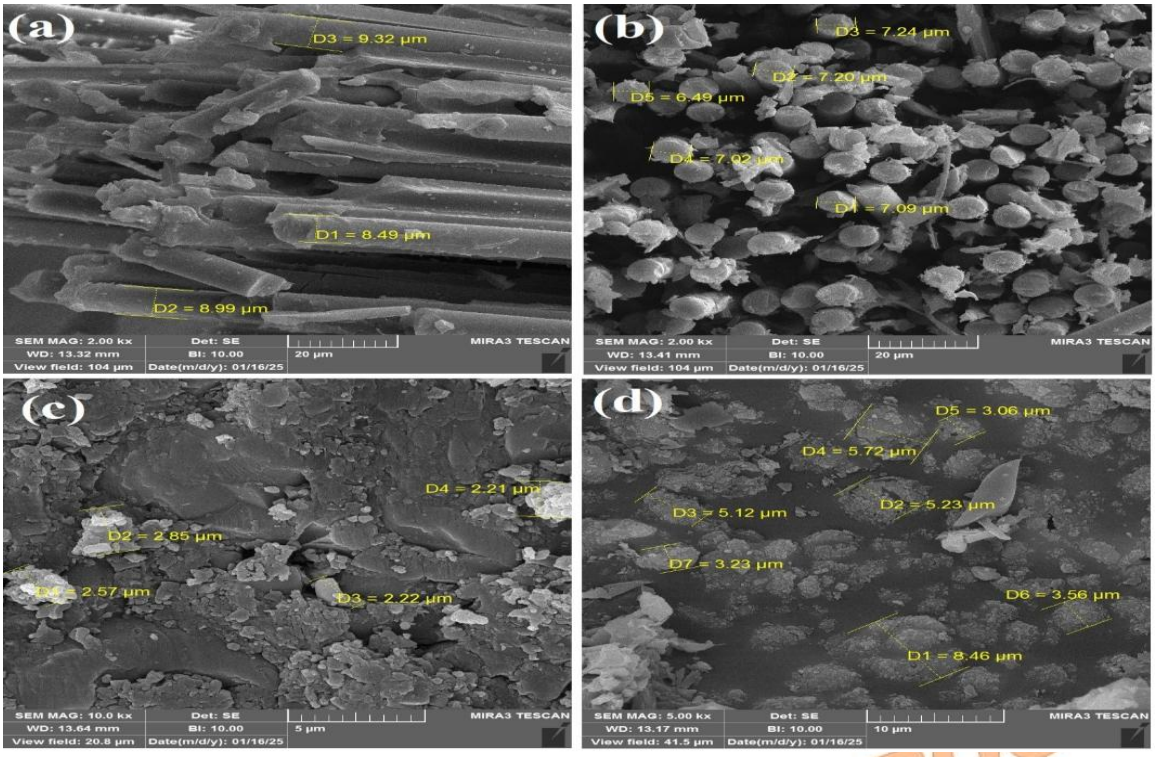

Fig. 4. (a) Highsilica/fiber diameter, (b) Carbon fiber diameter, (c) PTFE particles size, (d) SiC particles size

particles, forming a resin layer on their surfaces. Particles naturally bond together, creating larger aggregates due to the influence of interfacial forces. This tendency highlights the importance of these forces in shaping the behavior and properties of materials.

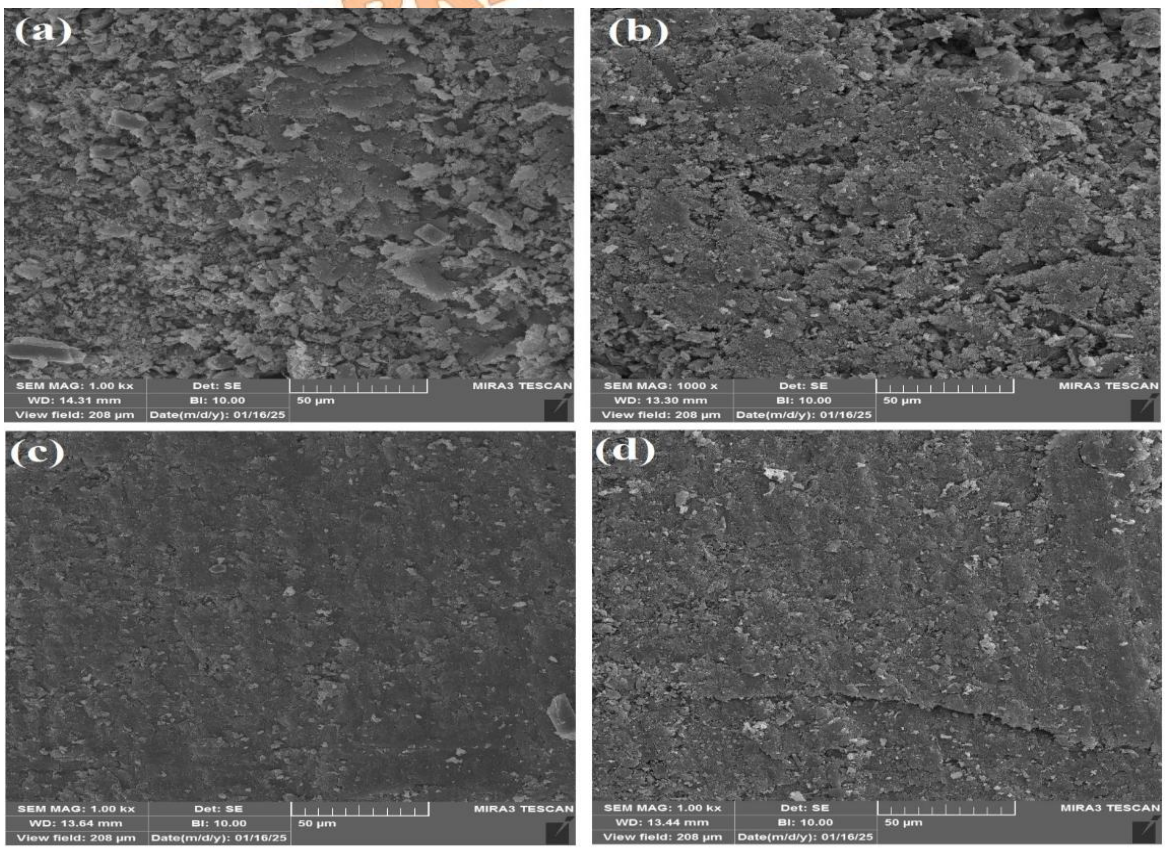

Fig. 3. (a) Highsilica/non particle, (b) Carbon-Highsilica/non particle, (c) Highsilica/10%wt particle, (d) Carbon-Highsilica/10%wt particle

4.2. DSC Thermal Test

DSC (Differential Scanning Calorimetry) analysis is an effective method for measuring heat flow from a sample as a function of temperature or time. In this study, we selected 6 samples from 14 fabricated ones and pure resole phenolic for thermal analysis. Table 4 and Fig. 5 present the glass transition temperature (Tg) and DSC curves for these selected samples.

The glass transition temperature (Tg) values presented in Table 4 were determined from DSC thermograms using the midpoint of the inflection on the heat flow curve. The samples analyzed were solid composite specimens after hot-press curing, ensuring that Tg corresponds to the crosslinked phenolic matrix.

While the application of glass transition temperature in thermoset composites is not as straightforward as in thermoplastic polymers, Tg can help assess the thermal stability of composites and the degree of crosslinking in thermoset materials [٤2]. As shown in Table 4, the addition of SiC-PTFE particles to the composites resulted in a relatively increased Tg. The most significant increase was observed in carbon composites, where the Tg of carbon composites containing 10% by weight of reinforcing particles rose by 5.4% compared to those without reinforcing particles. This enhancement is attributed to the presence of SiC and PTFE particles, both of which possess excellent thermal properties. SiC particles can serve as limiting points for the movement of polymer chains, requiring more energy for chain movement and thus raising the glass transition temperature [٤٢]. Furthermore, the influence of reinforcing particles on the glass transition temperature of composites indicates that a relatively strong interaction has occurred between the particles and the polymer matrix, as confirmed by the microscopic images in Fig. ٣. This interaction suggests that the presence of these particles can enhance the thermal stability of phenolic-based composites at elevated temperatures.

Table ٤. Results of samples with Tg

Sample	Tg(°C)
Pure Resole Phenolic	٨١.٥
Highsilica/0% particle	82.7
Highsilica/10% particle	83.7
Carbon/0% particle	87.8
Carbon/10% particle	92.5
Carbon-Highsilica/0% particle	86.7
Carbon-Highsilica/10% particle	88.3

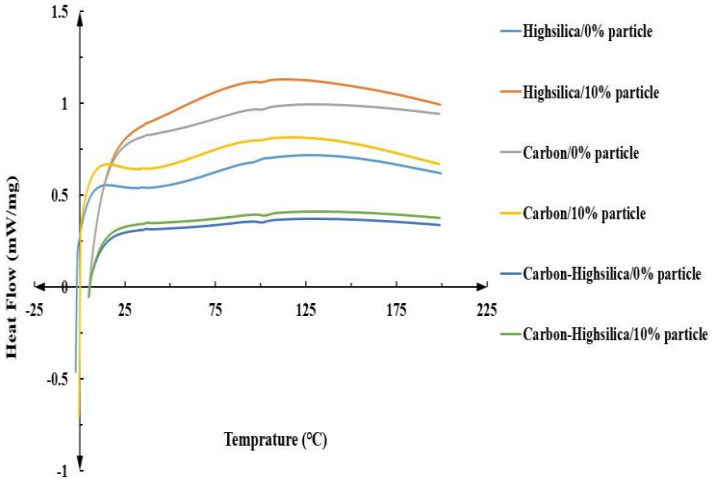

Fig. 5. DSC Curve of 6 Samples

4.3. Mechanical Tensile and Flexural Tests

Table 5 presents tensile and flexural strength/modulus for 14 samples, comprising 5 high-silica, 4 carbon, and 5 carbon-high-silica fiber composites.

4.3.1. *Effect of Fibers on Tensile Strength*

As summarized in Table 5, carbon fiber composites exhibited the highest tensile strength and modulus, reaching up to 264.8 MPa (sample 3). This value is 185% higher than that of the best-performing high-silica composite (sample 4, 93.0 MPa) and approximately 13% higher than the best hybrid carbon-high-silica system (sample 6, 235.2 MPa). The superior tensile performance of carbon laminates is attributed to the inherently higher strength of carbon fibers and their better interfacial interaction with phenolic resin, which enables more effective stress transfer during loading.

4.3.2. *Effect of Additive Particles on Tensile Strength*

The incorporation of particles significantly improved tensile properties across all fiber systems. For instance, the addition of 10 wt% SiC/PTFE particles to high-silica composites increased strength by ~38% (sample 4 vs. sample 1). Similarly, the addition of 10 wt% SiC/PTFE particles to carbon fiber composites showed ~22% improvement (sample 7 vs. sample 12), while hybrid laminates achieved up to 47% gain (sample 6 vs. sample 13). This enhancement is primarily attributed to the reinforcing role of SiC particles, which promote stress transfer and reduce crack propagation [25, 27]. SEM analysis confirmed a uniform dispersion of SiC in the

resin, supporting this improvement. Although PTFE is primarily included for thermal/abrasion resistance, when well-dispersed, it also contributes to mechanical enhancement, consistent with reports in the literature [21]. However, if these particles can effectively interact with the matrix, they may also positively influence mechanical properties [44], as observed in this study. Notably, previous research indicates that when SiC particles are utilized alongside other reinforcing particles in a hybrid form, the mechanical properties of the materials are further improved [45].

4.3.3. *Effect of Fibers on Flexural Strength*

In flexural loading, hybrid carbon–high-silica laminates outperformed other systems. The maximum flexural strength was observed in sample 6 (219.9 MPa), which is ~75% greater than carbon composites (sample 3, 127.7 MPa) and ~250% greater than high-silica composites (sample 4, 87.8 MPa).

During flexural loading, compressive stresses act on the upper surface and tensile stresses on the lower surface of the laminates. Hybrid carbon–high-silica systems exhibited superior performance because stress transfer between alternating fiber layers was more gradual, reducing stress concentration and delaying failure. The symmetric stacking sequence further enhanced interlaminar load sharing, resulting in the highest flexural strength and modulus observed in this study, which is consistent with previous reports on the benefits of hybrid fiber architectures [٤6–48].

4.3.4. *Effect of Additive Particles on Flexural Strength*

Similar to the tensile test results, the flexural strength in the flexural test is typically increased by adding reinforcing particles to the samples, as shown in previous studies [٢٤].

Figure 6 presents the tensile strength and flexural strength diagrams for 14 samples. The carbon fiber samples not only exhibit higher tensile strength but also demonstrate a greater fracture strain compared to the other samples. Similarly, the carbon-highsilica fiber samples show both higher flexural strength and ultimate fracture strain than the other samples.

In the stress-strain diagrams reflecting tensile strength, all samples fractured after reaching the yield point, with no discernible plastic region evident. This suggests that the reinforcing particles have not significantly influenced the ductility of the composites. Given that the polymer matrix displays brittle behavior, it is unrealistic to expect the particles to contribute to toughness. The presence of particles can only increase the area under the fracture curve and make it tougher in a way.

The flexural diagrams reveal that the composite samples with carbon-highsilica fibers exhibited greater strain and elongation after initial failure than those with only carbon fibers or highsilica fibers. Additionally, the area under the diagram for the carbon-highsilica fiber samples is larger than that of the carbon or highsilica fiber samples, indicating that these composites can withstand flexural stress for a longer duration.

4.4. *Analyzing Results Using Response Surface Methodology*

4.4.1. *Tensile Test*

An analysis of the results using Design-Expert software indicates that a first-order linear model is optimal for predicting tensile strength, as shown in Table 6. The model's p-value is less than 0.05, setting it apart from the other two models presented in the same table. The results of the ANOVA (Analysis of Variance) for this predicted linear model are detailed in Table 7. From this analysis, it is evident that the temperature parameter (T) lacks sufficient validity for predicting tensile strength, as indicated by a p-value greater than 0.05. In contrast, the other two parameters—weight percentage (Pw) and fiber type (F)—demonstrate strong validity in determining the tensile strength response according to the ANOVA optimization method. This suggests that the tensile behavior of the material is more significantly influenced by the composition of the fibers and reinforcing particles.

The regression models for tensile strength were developed in both actual and coded forms. Actual equations (Eqs. 2–4) describe the effect of particle content (P_w) and curing temperature (T) for each fiber type (Eq. 2 for carbon, Eq. 3 for high-silica, and Eq. 4 for hybrid). The coded equation (Eq. 5) combines all factors, where F_1 and F_2 are dummy variables representing carbon and hybrid fibers, respectively, while high-silica is considered the baseline.

Figure 7 displays both two-dimensional (2-D) and three-dimensional (3-D) response surface plots of tensile strength, illustrating how tensile strength values depend on particle weight percentage and temperature. Additionally, the average results for the fibers are presented in Fig. 7(b). The 2-D plot indicates that tensile strength increases as the particle weight percentage rises, although the influence of fiber type on tensile strength is greater than that of the particles. The optimal tensile strength is achieved when the weight percentage of reinforcing particles is 10%,

and carbon fibers are used as the primary reinforcement.

Table 5. Tensile and flexural properties of phenolic composites with different fibers and particle contents

Sample	Code	Tensile strength (MPa)	Tensile modulus (MPa)	Flexural strength (MPa)	Flexural modulus (MPa)
#	Neat Phenolic	۴۵.۴۸ ±1.8	۲۷۰۸.۹۹ ±81.9	۵۶.۶۵ ±2.4	۱۸۵۴.۳۲ ±56.8
1	Highsilica/180/0	67.03 ±2.7	1031.30 ±31.3	73.83 ±2.8	2461.03 ±94.3
2	Highsilica/140/0	62.39 ±1.6	1039.83 ±37.2	69.58 ±2.9	1739.51 ±62.8
3	Carbon/180/5	256.05 ±8.4	1969.61 ±59.4	127.74 ±8.5	4258.19 ±138.8
4	Highsilica/180/10	93.01 ±3.3	1860.21 ± 66.8	87.79 ±3.2	۴۳۸۹.۲۳ ±173.7
5	Carbon-Highsilica/140/10	204.68 ±6.1	4651.81 ±120.2	173.13 ±4.3	8656.50 ±290.9
6	Carbon-Highsilica/180/10	235.16 ±5.9	5225.77 ±147.7	219.86 ±9.5	10993.43 ±356.2
7	Carbon/160/10	264.79 ±7.6	6304.50 ±240.1	120.06 ±3.1	۶۰۰۳.۶۱ ±195.3
8	Carbon-Highsilica/140/0	168.74 ±4.2	3245.19 ±97.2	115.87 ±2.9	5793.51 ±174.4
9	Carbon/140/5	249.98 ±10.3	4098.03 ±123.3	101.96 ±2.4	5098.98 ±165.1
10	Highsilica/160/5	88.26 ±6.3	1260.85 ±88.5	87.83 ±3.5	4390.49 ±142.2
11	Highsilica/140/5	81.15 ±2.1	1399.13 ±69.2	72.83 ±1.8	۳۶۴۱.۲۵ ±119.6
12	Carbon/160/0	216.14 ±8.4	4322.87 ±130.4	110.41 ±3.8	5520.54 ±194.8
13	Carbon-Highsilica/180/0	157.89 ±4.7	3157.83 ±95.6	142.01 ±4.6	7100.65 ±233.5
14	Carbon-Highsilica/140/5	186.84 ±4.5	3892.52 ±117.4	154.28 ±7.7	7714.33 ±182.2

Table 6. Model Analysis for Tensile Strength

Source	Sequential p-value	Adjusted R^2	Predicted R^2	R^2	
Linear	< 0.0001	0.9722	0.9471	0.9808	Suggested
2FI	0.6496	0.9668	0.7552		
Quadratic	0.2786	0.9815	0.8023		
Cubic					Aliased

Table 7. ANOVA analysis for Linear model

Factor	Sum of Squares	Mean Square	F-value	p-value
P_w	4651.11	4651.11	28.38	0.0005
T	1.54	1.54	0.0094	0.9248
F	65599.98	32799.99	200.13	< 0.0001
Residual	1475.03	163.89		

$$\sigma_T = 225.277 + 4.622P_w + 0.019T \quad (2)$$

$$\sigma_T = 56.838 + 4.622P_w + 0.019T \quad (3)$$

$$\sigma_T = 164.585 + 4.622P_w + 0.019T \quad (4)$$

$$\sigma_T = 175.05 + 23.11P_w + 0.38T + 76.38F_1 - 92.06F_2 \quad (5)$$

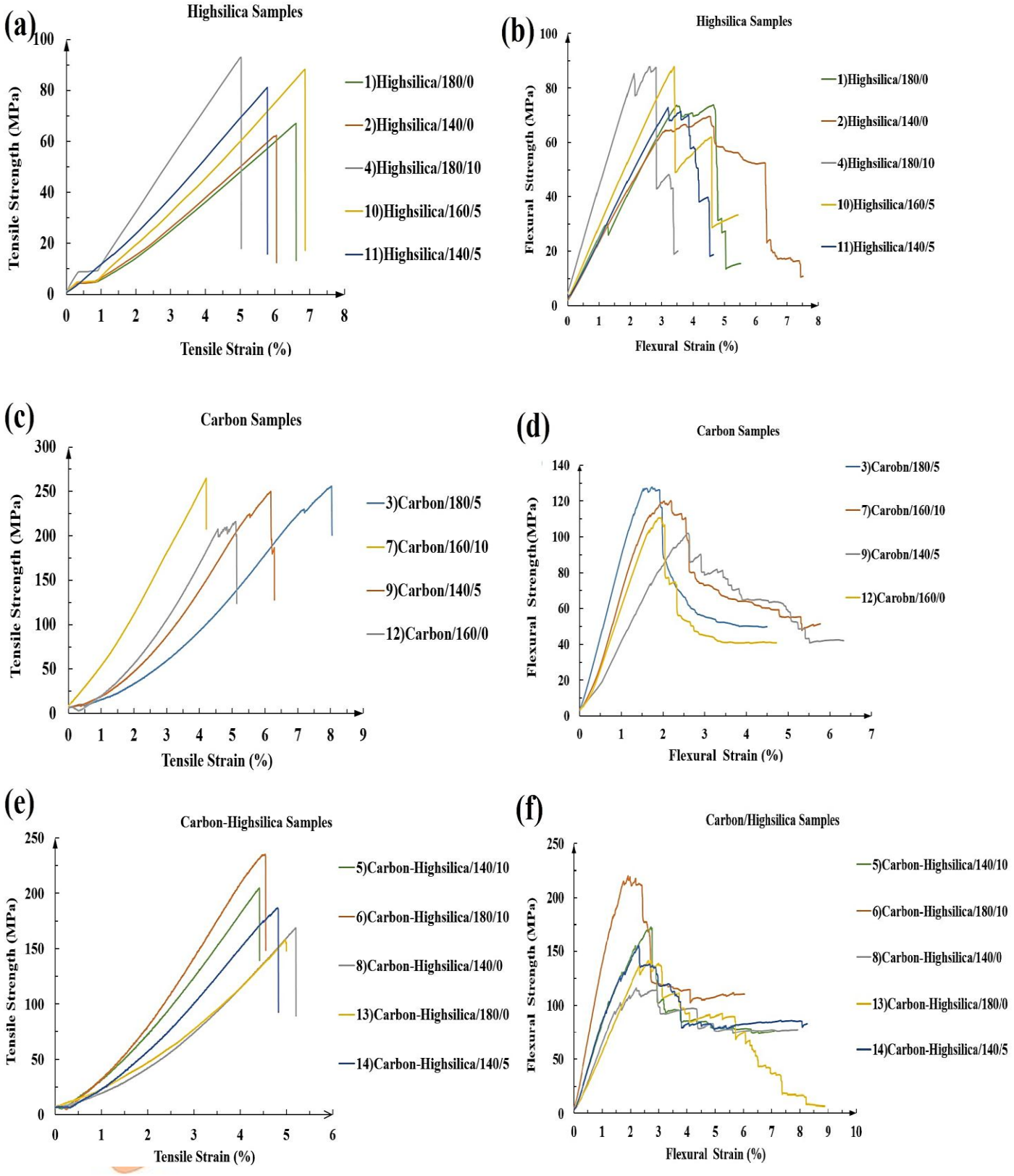

Fig. 6. (a) Highsilica samples tensile curves, (b) Highsilica samples flexural curves, (c) Carbon samples tensile curves, (d) Carbon samples flexural curves, (e) Carbon-Highsilica samples tensile curves, (f) Carbon-Highsilica samples flexural curves

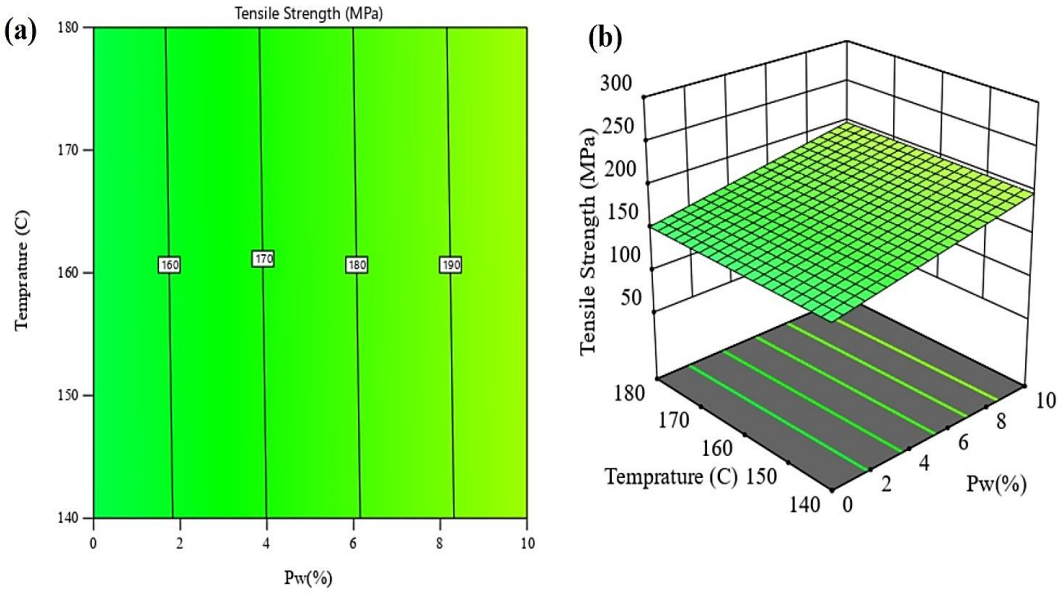

Fig. ٧. (a) 2D Model Response surface methodology for tensile strength, (b) 3D Model Response surface methodology for tensile strength

4.4.2. Flexural Test

The analysis of the flexural strength results, conducted using Design-Expert software, indicates that a quadratic model is appropriate, as shown in Table 8. The results of the ANOVA for the predicted model are presented in Table 9. In examining the parameters that influence flexural strength, it is noted that the p-values for all parameters—weight percentage (Pw), temperature (T), and fiber type (F)—are less than 0.05. This indicates that all three parameters, along with their interactions, have sufficient validity in the data analysis of the variance optimization method. According to Table 9, the interaction effects among the parameters are significant, particularly the interaction between weight percentage and fiber type, which has a p-value of 0.002. Furthermore, the quadratic terms are also important in this model, indicating that the relationship between the input parameters and flexural strength is not entirely linear. Flexural strength was modeled using both actual and coded equations. Actual equations (Eq. 6 for carbon, Eq. 7 for highsilica and Eq. 8 for hybrid) capture the influence of P_w and T for each fiber type, while the coded equation (Eq. 9) integrates all factors.

Figure 8 displays both two-dimensional and three-dimensional response surface plots of flexural strength, illustrating the relationship between flexural strength, the weight percentage of particles, and temperature. Note that the average results obtained for the fibers are included in Fig. ٨(b). The two-dimensional plot indicates that as the weight percentage of reinforcing particles increases, the flexural strength also rises. Additionally, temperature plays a significant role in affecting flexural strength.

The optimal combination for achieving maximum flexural strength is at 180°C with a 10% weight percentage of carbon-highsilica hybrid fibers. The three-dimensional plot highlights that curing temperature has a more substantial impact on flexural strength compared to tensile strength. Moreover, the interaction between the weight percentage of particles and fiber type is quite pronounced, suggesting that each type of fiber responds differently to specific amounts of reinforcing particles.

Table 8. Model Analysis for Flexural Strength

Source	Sequential p-value	Adjusted R^2	Predicted R^2	R^2	
Linear	0.0002	0.8483	0.7031		
2FI	0.0222	0.9747	0.8984		
Quadratic	0.0200	0.9990	0.9887	0.9998	Suggested
Cubic					Aliased

Table 9. ANOVA analysis for the Quadratic model

Factor	Sum of Squares	Mean Square	F-value	p-value	
Model	23878.61	2170.78	1166.41	0.0009	significant
P_w	3063.27	3063.27	1645.96	0.0006	
T	1374.36	1374.36	738.47	0.0014	
F	14450.29	7225.14	3882.23	0.0003	
P_w T	148.70	148.70	79.90	0.0123	
P_wF	1864.32	932.16	500.87	0.0020	
TF	194.82	97.41	52.34	0.0187	
P_w^2	130.42	130.42	70.08	0.0140	
T^2	96.85	96.85	52.04	0.0187	
Residual	3.72	1.86			

$$\sigma_F = -439.77 - 4.49P_w + 6.49T + 0.05P_wT - 0.31{P_w}^2 - 0.01T^2 \quad (6)$$

$$\sigma_F = -429.66 - 5.18P_w + 6.24T + 0.05P_wT - 0.31{P_w}^2 - 0.019T^2 \quad (7)$$

$$\sigma_F = -452.99 + 1.29P_w + 6.74T + 0.05P_wT - 0.31{P_w}^2 - 0.019T^2 \quad (8)$$

$$\sigma_F = 129.9 + 13.33P_w + 12.85T - 7.12F_1 - 41.51F_2 + 5.37P_wT - 8.51P_wF_1 - 11.94P_wF_2 + 0.04TF_1 - 5.09TF_2 - 7.84{P_w}^2 - 7.65T^2 \quad (9)$$

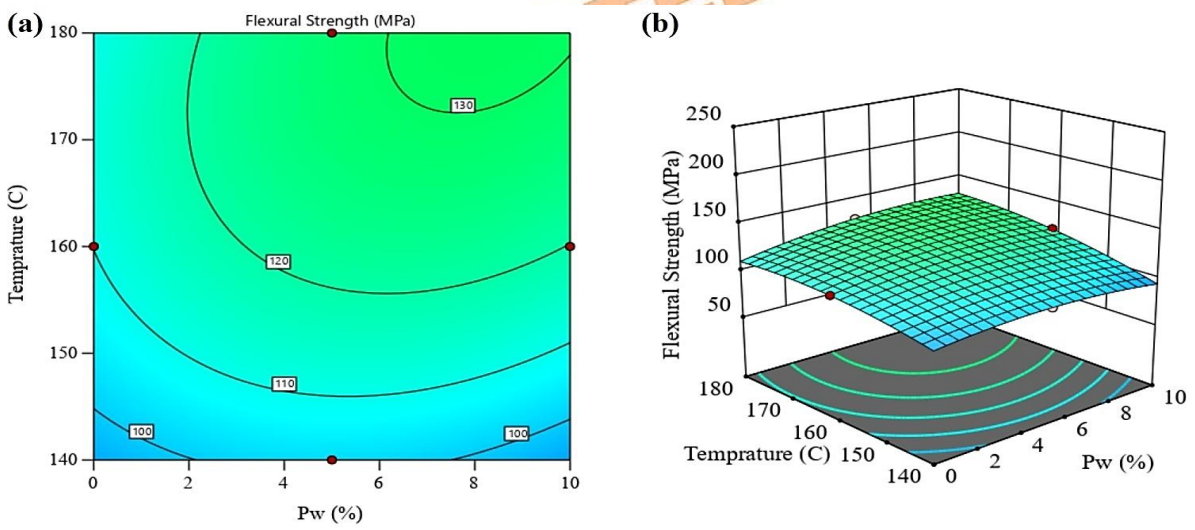

Fig. 8. (a) 2D Model Response surface methodology for flexural strength, (b) 3D Model Response surface methodology for flexural strength

4.4.3. Diagnostics and Optimization

Diagnostics of the Models

Since two different models were selected for tensile and flexural responses (first-order linear model for tensile strength and quadratic model for flexural strength), separate diagnostic checks were performed to evaluate their statistical adequacy. The diagnostic analysis of the tensile strength model is presented in Fig. 9(a). Here, the

The normal probability plot of residuals also demonstrates that the residuals follow a near-linear trend along the reference line, indicating that the assumption of normality is satisfied. No major outliers or systematic deviations were observed. Although a linear model was selected as the best fit, its adequacy is further confirmed by this diagnostic analysis. According to ANOVA,

tensile strength is predominantly controlled by powder content and fiber type, while curing temperature did not have a significant effect. This explains why a linear model was sufficient: the tensile response is governed mainly by direct effects of material composition rather than complex interactions or curvature. The residuals pattern further indicates that the model captures the systematic variability well, with random scatter consistent with experimental error.

Also, the normal probability plot of residuals for flexural strength is shown in Fig. 9(b). The majority of the residuals lie very close to the reference straight line, confirming that the error terms follow an approximately normal distribution. Only a single observation deviated from the line at the upper tail, which can be considered a mild outlier. However, this deviation is not sufficient to compromise the model's adequacy. The good alignment of the residuals supports the reliability of the quadratic model in describing the flexural response. The fact that flexural strength required a quadratic model is consistent with its sensitivity to the combined influence of powder content and curing temperature, which creates interaction and curvature effects that cannot be captured by a linear model alone.

Together, these diagnostics confirm that the selected models are statistically valid and appropriately reflect the physical behavior of the system. Flexural strength requires a quadratic model due to interaction and curvature effects, whereas tensile strength is adequately described by a linear model driven by main compositional factors.

Multi-Response Optimization

The multi-response optimization was conducted using the desirability function to maximize both tensile and flexural strengths simultaneously. The software generated up to 100 possible solutions, each corresponding to different combinations of powder content, curing temperature, and fiber type. Among these, one representative solution with high desirability was selected. This condition corresponded to 3 wt% powder content, a curing temperature of 170 °C, and carbon/high-silica fiber reinforcement with an overall desirability close to D = 1.000. Under these settings, the models predicted a tensile strength of ~181 MPa and a flexural strength of ~170 MPa. One of the optimization plots for this solution is presented in Fig. 10. In these figures, the Actual factor denotes the fixed fiber type (carbon/high-silica), while the response surfaces display the effects of powder content and curing temperature.

This solution demonstrates that even at relatively low filler content, simultaneous improvement of tensile and flexural responses can be achieved through appropriate selection of fiber type and curing parameters. Including these optimization plots in the manuscript ensures transparency of the modeling process.

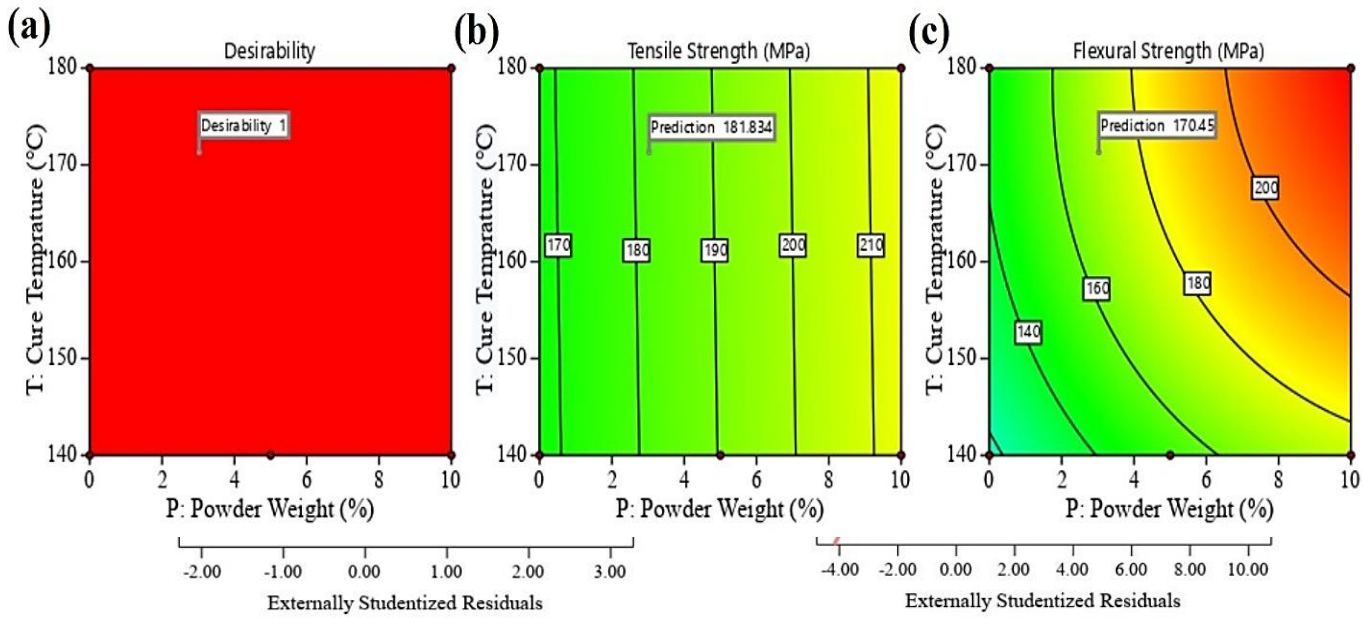

Fig. 9. (a) Normal probability plot of residuals for tensile strength b) Normal probability plot of residuals for flexural strength

4.4.4. Validation of Mathematical Models

The comparison of experimental data from mechanical tests, specifically tensile and flexural tests, with predicted data from the ANOVA formulation is illustrated in a graph relative to the 45-degree diagonal line. The closer the data points are to this diagonal line, the greater the agreement between the experimental and predicted data. This proximity enhances the accuracy of the final results and validates the research findings. To provide a clearer understanding of this agreement, Fig. 11 displays graphs of the experimental (actual) and predicted values for the two mechanical properties: tensile strength and flexural strength. Additionally, a comparison of the root mean square error (RMSE) values in the ANOVA tables with the experimental-predicted graphs indicates a strong correspondence between the residual values and the experimental data for both tensile strength and flexural strength. To provide a quantitative assessment, statistical measures have been calculated based on the ANOVA results. For tensile strength, the RMSE is approximately 12.8 MPa, derived from the residual mean square ($\sqrt{163.89}$) reported in Table 7, which reflects a relative error of 5-10% compared to the mean experimental tensile strength (approximately 178 MPa across samples). For flexural strength, the RMSE is approximately 1.36 MPa, calculated from the residual mean square ($\sqrt{1.86}$) in Table 9, corresponding to a relative error of less than 2% relative to the mean experimental flexural strength (approximately 121 MPa). These error ranges are within acceptable limits for Response Surface Methodology (RSM) studies in composite materials. Also, the D-optimal design achieved a D-efficiency of 85%, ensuring efficient parameter estimation .Furthermore, suppose the difference between the predicted correlation coefficient (R^2 Predicted) and the adjusted correlation coefficient (R^2 Adjusted) is less than 0.2. In that case, we can conclude that the experimental and predicted results are in close agreement with only a minor difference. Moreover, models that exhibit a high correlation with experimental data can be effectively used to predict mechanical properties. For tensile strength and flexural strength, the correlation coefficients were calculated as R^2 = 0.9808 and R^2 = 0.9998, respectively. These values indicate the high accuracy of the linear model for tensile strength and the quadratic model for flexural strength, demonstrating that these models accurately represent the experimental data [49].

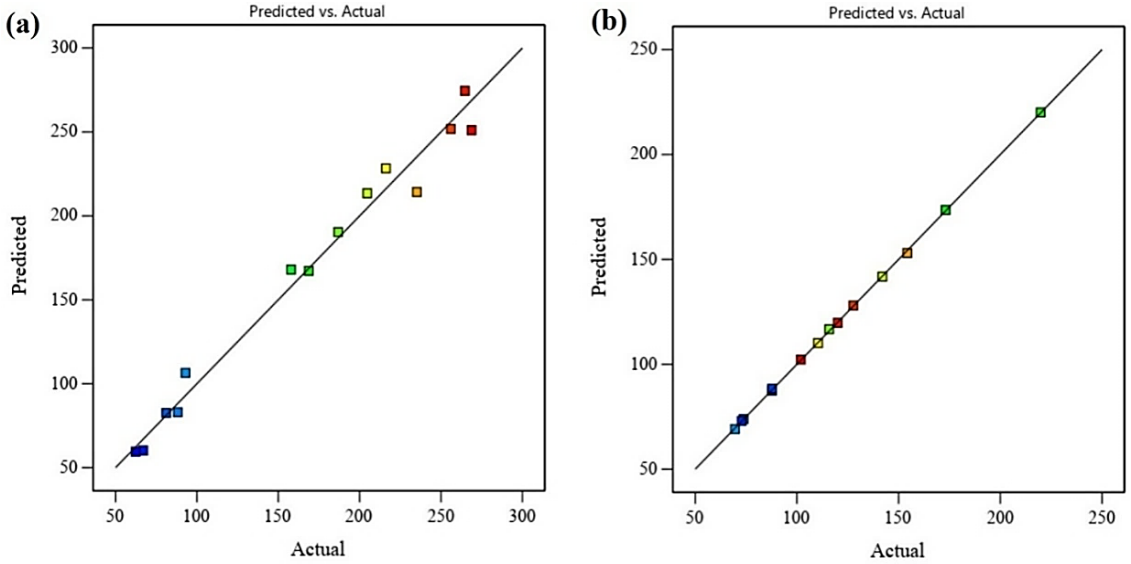

Fig. 11. (a) Comparison of experimental and predicted data for a) tensile strength b) flexural strength relative to the diagonal line 45°

5. Conclusion

In this study, a hybrid composite was fabricated using two types of carbon fibers, high-silica fibers, and reinforcing particles made of silicon carbide (SiC) and polytetrafluoroethylene (PTFE). The response surface methodology was employed to optimize manufacturing variables, focusing on three key parameters: particle weight percentage, curing temperature, and fiber type. Scanning electron microscopy results indicated that the composites failed primarily in the fiber area. Additionally, PTFE and SiC additive particles interacted relatively well with the resin, effectively.

preventing crack propagation. Differential scanning calorimetry results demonstrated that the incorporation of reinforcing particles improved the glass transition temperature, enhancing the thermal stability of the composite. Tensile strength results, along with analysis of

variance utilizing a first-order model, revealed that the curing temperature did not have a significant impact on the tensile strength. In contrast, the fiber type and particle weight percentage were found to be critical factors. Notably, using carbon fibers with a 10% weight percentage of reinforcing particles yielded the best results. Also, the analysis of ANOVA showed that all three parameters—weight percentage (Pw), temperature (T), and fiber type (F)—significantly influenced flexural strength, with interactions between them playing an important role. The optimal combination for flexural strength was identified as a curing temperature of 180°C, a weight percentage of 10%, and the use of hybrid carbon-highsilica fibers. For industrial production of phenolic composites with enhanced tensile properties, a formulation of 10 wt% SiC/PTFE particles, cured at 180°C for hours under 150 psi pressure with carbon fiber reinforcement, is recommended. For superior flexural performance, the same particle loading and curing conditions should be adopted for carbon/high-silica hybrid fibers. Furthermore, the response surface methodology models developed in this study demonstrated high accuracy in predicting mechanical properties, indicating that this approach can effectively optimize the properties of composites by considering various parameters.

Funding Statement

The authors did not receive support from any organization for the submitted work.

Conflict of interest

The authors have no competing interests or conflicts of interest to declare that are relevant to the content of this article.

References

[١] Mazumdar, S., 2001. Composites manufacturing: materials, product, and process engineering. CRC Press

[٢] Gardziella, A., Pilato, L.A. and Knop, A., 2013. Phenolic resins: chemistry, applications, standardization, safety, and ecology. *Springer Science & Business Media.*

[٣] Jawaid, M. and Asim, M., 2021. Phenolic polymers-based composite materials. Springer.

[٤] Rogers, M.E., Long, T.E. and Turner, S.R., 2003. Introduction to synthetic methods in step-growth polymers. *Synthetic Methods in Step-Growth Polymers*, pp. 1–16.

[٥] Burkhart, T., Oberressl, P. and Oldring, P., 1998. The chemistry and application of phenolic resins or phenolplasts. *Wiley.*

[٦] Ratna, D., 2009. Handbook of Thermoset Resins. *iSmithers Shawbury, UK.*

[٧] Gouda, P.S., Kodancha, K.G. and Siddaramaiah, D.J., 2013. Experimental and numerical investigations on fracture behavior of high silica glass/satin textile fiber reinforced hybrid polymer composites. *Advanced Materials Letters*, 4(11), pp. 827–835.

[٨] Wei, Q.H., Wang, C.H., Wang, H.S., Li, L., Shao, C.T. and Dong, B., 2014. Study on process and properties of needling silica fiber reinforced silica composites. *Advanced Materials Research*, 833, pp. 146–149.

[٩] Li, Z., Zheng, R. and Li, L., 2013. Experimental investigation on heat-resistant layer of high silica phenolic composites in ramjet chamber. *Journal of Propulsion Technology*, 34(1), pp. 76–80.

[١٠] Feng, B., Wang, X., Wu, Z., Yang, Y. and Pan, Z., 2021. Performance of anchorage assemblies for CFRP cables under fatigue loads. *Structures*, 29, pp. 947–953.

[١١] Guo, R., Li, C. and Xian, G., 2023. Water absorption and long-term thermal and mechanical properties of carbon/glass hybrid rod for bridge cable. *Engineering Structures*, 274, p. 115176.

[١٢] Afshar, A., Mihut, D. and Chen, P., 2020. Effects of environmental exposures on carbon fiber epoxy composites protected by metallic thin films. *Journal of Composite Materials*, 54(2), pp. 167–177.

[١٣] Rahmani, H., Najafi, S.H.M. and Ashori, A., 2014. Mechanical performance of epoxy/carbon fiber laminated composites. *Journal of Reinforced Plastics and Composites*, 33(8), pp. 733–740.

[١٤] Wang, D.Y., 2016. Novel fire retardant polymers and composite materials. *Woodhead Publishing.*

[15] Ghiaskar, A. and Nouri, M.D., 2023. Investigating fracture behavior and

energy absorption of flexible hybrid biocomposites with soft–hard rubber/biofiller layers and fabric impregnated with matrix under high-velocity impact. *Journal of the Brazilian Society of Mechanical Sciences and Engineering*, 45(11), p. 585.

[16] Ghiaskar, A. and Taghipoor, H., 2024. Investigating mechanical properties and energy absorption of elastomeric polymer nanocomposites containing cellulose nanofibers in tensile, quasi-static compression, and high strain rate tests. *Physica Scripta*, 99,(8), p. 085963.

[17] Ghiaskar, A. and Nouri, M.D., 2023. A novel flexible biocomposite with hemp woven fabric and natural rubber based on lignin green filler: investigation numerical and experimental under high-velocity impact. *Physica Scripta*, 98(10), p. 105307.

[18] Ghiaskar, A. and Nouri, M., 2022. High-velocity impact behavior of lignin/NR/hemp green composite: a comparative study. *Journal of the Brazilian Society of Mechanical Sciences and Engineering*, 44, pp. 1–20.

[19] Hasanzadeh, I., Eskandari, M.J. and Daneshmand, H., 2022. Polyurethane acrylate/multiwall carbon nanotube composites as temperature and gas sensors: Fabrication, characterization, and simulation. *Diamond and Related Materials*, 130, p. 109484.

[٢٠] Mouritz, A.P. and Gibson, A.G., 2007. Fire properties of polymer composite materials. *Springer Science & Business Media.*

[٢١] Zhang, H. et al., 2022. Comparative study on the mechanical, tribological, and thermal properties of POM composites filled with different PTFE. *Journal of Thermoplastic Composite Materials*, 35(9), pp. 1319–1341.

[٢٢] Panin, S. et al., 2020. The effect of annealing of milled carbon fibers on the mechanical and tribological properties of solid-lubricant thermoplastic polyimide-based composites. *Polymer Engineering & Science*, 60(11), pp. 2735–2748.

[٢٣] Basavaraj, E., Ramaraj, B. and Siddaramaiah, 2012. Investigations on the influence of polytetrafluoroethylene powder as a filler on physico-mechanical and wear characteristics of nylon 66/graphite composites. *High Performance Polymers*, 24(7), pp. 616–624.

[٢٤] Daneshmand, H., Eskandari, M.J. and Araghchi, M., 2023. Reinforced PTFE composites with atomized powder of Inconel 625 alloy for sealing application: Study of structural properties and molecular dynamics simulation. *Materials Today Communications*, 35, p. 10641.

[٢٥] Bera, T., Sethi, R.R. and Mohanty, S., 2024. Effect of silicon carbide particles on the mechanical, thermal and structural properties of recycled high-density polyethylene. *Plastics, Rubber and Composites*, 53,(1), pp. 53–67.

[٢٦] Kumaresan, K., Chandramohan, G., Senthilkumar, M. and Suresha, B., 2012. Dynamic mechanical analysis and wear of carbon–epoxy composite filled with SiC. *Journal of Reinforced Plastics and Composites*, 31(21), pp. 1435–144.

[٢٧] Basingala, P.K. and Neigapula, V.S.N., 2024. Enhancement of mechanical and thermal properties of carbon fiber phenolic resin composites using silicon carbide filler for thermal protection system applications. *Journal of Industrial Textiles*, 54, pp. 1528083724126331.

[٢٨] Kasmaei, M.P.J., Alaei, M.H., Jam, J.E. and Soltani, S.A.K., 2024. Effect of SiC dominated with ZrB2 particles on the ablation and mechanical properties of carbon/novolac-epoxy (EPN1180) composite at 3000° C. *Polymer Composites*, 45(17), pp. 15574–15589.

[٢٩] Lamidi, S., Olaleye, N., Bankole, Y., Obalola, A., Aribike, E. and Adigun, I., 2022. Applications of response surface methodology (RSM) in product design, development, and process optimization. IntechOpe.

[٣٠] Albooyeh, A., Soleymani, P. and Taghipoor, H., 2022. Evaluation of the mechanical properties of hydroxyapatite-silica aerogel/epoxy nanocomposites: optimizing by

response surface approach. *Journal of the Mechanical Behavior of Biomedical Materials*, 136, p. 105513.

[٣١] Myers, R.H., Montgomery, D.C. and Anderson-Cook, C.M., 2016. *Response Surface Methodology:* Process and Product Optimization Using Designed *Experiments. John Wiley & Sons.*

[٣٢] Akintunde, A.M., Ajala, S.O. and Betiku, E., 2015. Optimization of Bauhinia monandra seed oil extraction via artificial neural network and response surface methodology: a potential biofuel candidate. *Industrial Crops and Products*, 67, pp. 387–394.

[٣٣] Okeleye, A.A. and Betiku, E., 2019. Kariya (Hildegardia barteri) seed oil extraction: comparative evaluation of solvents, modeling, and optimization techniques. *Chemical Engineering Communications*, 206(9), pp. 1181–1198.

[٣٤] Daneshpayeh, S., Ghasemi, F.A. and Ghasemi, I., 2017. Mechanical Properties of Nanocomposites Based on Polypropylene-Linear Low Density Polyethylene-Titanium Dioxide Nano Particles by Response Surface Methodology. *Journal of Tabriz Mechanical Engineering*, 7(7), pp. 903–101.

[٣٥] Yaghoobi, H. and Fereidoon, A., 2018. Modeling and optimization of tensile strength and modulus of polypropylene/kenaf fiber biocomposites using Box–Behnken response surface method. *Polymer Composites*, 39, pp. E463–E479.

[٣٦] Cantwell, W.J. and Morton, J., 1991. The impact resistance of composite materials—a review. *Composites*, 22(5), pp. 347–362.

[٣٧] Jeon, H. et al., 2017. A combined analytical formulation and genetic algorithm to analyze the nonlinear damage responses of continuous fiber toughened composites. *Computational Mechanics*, 60, pp. 393–408.

[٣٨] Ojha, S., Bisaria, H., Mohanty, S. and Kanny, K., 2024. Fractographic analysis of fiber-reinforced polymer laminate composites for marine applications: A comprehensive review. *Polymer Composites.*

[٣٩] Jollivet, T., Peyrac, C. and Lefebvre, F., 2013. Damage of composite materials. *Procedia Engineering*, 66, pp. 746–758

[٤٠] Heslehurst, R.B., 2014. Defects and Damage in Composite Materials and Structures. *CRC Press*.

[٤١] Talreja, R. and Singh, C.V., 2012. Damage and Failure of Composite Materials. *Cambridge University Press.*

[٤٢] Khan, A., Bhawani, S.A., Asiri, A.M. and Khan, I., 2018. Thermoset composites: preparation, properties and applications. *Materials Research Forum LLC.*

[٤٣] Melati, A., Settar, A., Chetehouna, K., Okur, N. and Berkalp, O.B., 2023. Experimental analysis of the effect of natural fibers and SiC filler on the thermal behavior of green biocomposites. *Journal of Applied Polymer Science*, 140(38), p. e54430.

[٤٤] Wang, X., Chi, Y. and Cao, Y., 2014. The Effect of PTFE on mechanical, friction and wear properties of CF/PMMA composites," *Journal of Thermoplastic Composite Materials*, 27(9), pp. 1232–1238.

[٤٥] Li, A., Wang, S., Chen, Z., Liu, H. and Wang, H., 2022. The synergistic effect of SiC/R-GO composite on mechanical and tribological properties of thermosetting polyimide. *Journal of Composite Materials*, 56(2), pp. 267–278.

[٤٦] Arumugam, S et al., 2020. Investigations on the mechanical properties of glass fiber/sisal fiber/chitosan reinforced hybrid polymer sandwich composite scaffolds for bone fracture fixation applications. *Polymers*, 12(7), p. 1501.

[٤٧] Dong, C., 2020. Flexural properties of symmetric carbon and glass fibre reinforced hybrid composite laminates. *Composites Part C: Open Access*, 3(1), p. 100047.

[٤٨] Kumar, M., Kumar, S., 2024. Short literature survey on fiber-reinforced hybrid composites.

Mechanics of Advanced Composite Structures, 11(2), pp. 425–452.

[٤٩] Gaitonde, V., Karnik, S., Davim, J. P., 2009. Some studies in metal matrix composites machining using response surface methodology. *Journal of Reinforced Plastics and Composites*, 28(20), pp. 2445–2457.